Available online at www.sciencedirect.com
ScienceDirect
Progress in Natural Science 19 (2009) 811–816
Progress in Natural Science
www.elsevier.com/locate/pnsc

SH-guided waves in layered piezoelectric/piezomagnetic plates

Guoquan Nie [a,b,*], Zijun An [a], Jinxi Liu [b]

[a] College of Mechanical Engineering, Yanshan University, Qinhuangdao 066004, China
[b] Department of Engineering Mechanics, Shijiazhuang Railway Institute, Shijiazhuang 050043, China

Received 12 August 2008; received in revised form 28 September 2008; accepted 8 October 2008

Abstract

The propagation of shear horizontal (SH) guided waves in a coupled plate consisting of a piezoelectric layer and a piezomagnetic layer is studied. Both the layers are transversely isotropic and perfectly bonded along the interface. The upper and the lower surfaces of the plate are assumed to be mechanically free, electrically open and magnetically closed. Two different cases are considered. One is that the bulk shear wave velocity of piezoelectric material is larger than that of piezomagnetic material. The other is that the bulk shear wave velocity of piezomagnetic material is larger than that of piezoelectric material. The dispersion relation is obtained while the phase velocity is among the bulk shear wave velocity of two different layers. The numerical results show that the phase velocity approaches the smaller bulk shear wave velocity of the material in the system with the increase in the wave number for different modes. The thickness ratio and the properties of the piezoelectric material have great effect on the dispersion behaviors. The results of this paper can offer some fundamental theory to the application of piezoelectric/piezomagnetic composites or structures.

Keywords: Piezoelectric material; Piezomagnetic material; SH-guided wave; Dispersion relation

1. Introduction

In recent years, non-destructive detection (NDT) using guide wave propagation in solid medium is widely applied. So signal processing, interaction of elastic waves with cracks, inhomogeneities and other defects in elastic media have been studied extensively [1–3]. The early research on the magnetoelectric effect of such composites was carried out by Van Suchtelen [4]. The result showed that the magnetoelectric coefficient in the $BaTiO_3$–$CoFe_2O_4$ composite is two orders larger than that of Cr_2O_3. Since their original works, especially in the last decades, the magnetoelectric effect of piezoelectric/piezomagnetic composites has been studied by many researchers [5–10].

Shear horizontal (SH) wave propagation in a layered system consisting of a layer bonded to a different semi-infinite substrate is of intensive research interest in recent years. Wang et al. [11] studied the Love wave propagation in a piezoelectric lamina bonded onto a semi-infinite metal medium and found that the phase velocities initiated at the shear wave velocity of the host medium tended towards the B-G surface wave velocity for the piezoelectric layer at high wave numbers for the first mode. Fan and Yang [12] analyzed the propagation behaviors of SH surface waves in a layered system consisting of a piezoelectric half-space and a metal or elastic dielectric layer with an imperfect interface and found that the dispersion characteristic of the wave was sensitive to the interface property. Du et al. [13] studied the Love wave propagation in a piezomagnetic layer bonded onto a piezoelectric half-space with initial stress, and the effects of the initial stress on the phase velocity and the magneto-electromechanical coupling factor are also discussed in detail. However, to the authors' knowledge, the substrate is assumed to be semi-infinite media in the published works, and the influence of the thickness

* Corresponding author. Tel.: +86 311 87936400; fax:+86 311 87936419.
E-mail address: Niegq@sjzri.edu.cn (G. Nie).

1002-0071/$ - see front matter © 2009 National Natural Science Foundation of China and Chinese Academy of Sciences. Published by Elsevier Limited and Science in China Press. All rights reserved.
doi:10.1016/j.pnsc.2008.10.007

of the substrate is not taken into consideration. The objective of this work is to present an exact solution for the SH-guided wave propagation in layered piezoelectric/piezomagnetic plates. The thickness ratio of the piezoelectric layer to the piezomagnetic layer is considered. The influences of piezoelectric material properties are also discussed.

2. Formulation of the problem

The geometry of the problem is shown in Fig. 1. The thicknesses of the piezoelectric layer and the piezomagnetic layer are d^e and d^m, respectively. Both the layers are transversely isotropic with the basal plane x_1–x_2 and perfectly bonded along the interface $x_2 = 0$.

For a SH-guided wave propagating in the x_1–x_2 plane, the anti-plane acoustic mode and the in-plane electromagnetic mode are coupled. The constitutive equations of the piezomagnetic layer and the piezoelectric layer can be expressed as follows [14]:

$$\begin{aligned} \sigma_{3\alpha}^m &= c_{44}^m \frac{\partial u_3^m}{\partial x_\alpha} + h_{15} \frac{\partial \psi^m}{\partial x_\alpha} \\ D_\alpha^m &= -\in_{11}^m \frac{\partial \varphi^m}{\partial x_\alpha} \qquad (\alpha = 1, 2) \\ B_\alpha^m &= h_{15} \frac{\partial u_3^m}{\partial x_\alpha} - \mu_{11}^m \frac{\partial \psi^m}{\partial x_\alpha} \end{aligned} \tag{1}$$

for the piezomagnetic layer and

$$\begin{aligned} \sigma_{3\alpha}^e &= c_{44}^e \frac{\partial u_3^e}{\partial x_\alpha} + e_{15} \frac{\partial \varphi^e}{\partial x_\alpha} \\ D_\alpha^e &= e_{15} \frac{\partial u_3^e}{\partial x_\alpha} - \in_{11}^e \frac{\partial \varphi^e}{\partial x_\alpha} \qquad (\alpha = 1, 2) \\ B_\alpha^e &= -\mu_{11}^e \frac{\partial \psi^e}{\partial x_\alpha} \end{aligned} \tag{2}$$

for the piezoelectric layer.

In Eqs. (1) and (2), u_3 and $\sigma_{3\alpha}$ are the components of displacement and stress, D_α and φ are the electric displacement and electric potential, B_α and ψ are the magnetic flux density and magnetic potential, c_{44}, e_{15}, and h_{15} are the elastic, piezoelectric and piezomagnetic constants, ε_{11} and μ_{11} are the dielectric permittivity and magnetic permeability, respectively. The superscripts "e" and "m" denote the quantities of piezoelectric and piezomagnetic materials, respectively.

In the usual quasi-static electromagnetic approximation, the governing equations of the piezomagnetic layer and the piezoelectric layer are given by

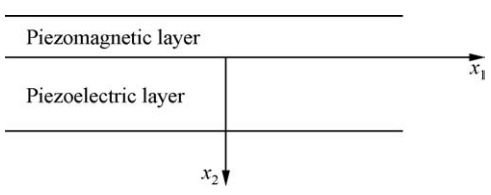

Fig. 1. Geometry of two-layered magnetoelectric plate.

$$\begin{aligned} &c_{44}^m \nabla^2 u_3^m + h_{15} \nabla^2 \psi^m = \rho^m \frac{\partial^2 u_3^m}{\partial t^2} \\ &\nabla^2 \varphi^m = 0 \\ &h_{15} \nabla^2 u_3^m - \mu_{11}^m \nabla^2 \psi^m = 0 \end{aligned} \tag{3}$$

$$\begin{aligned} &c_{44}^e \nabla^2 u_3^e + e_{15} \nabla^2 \varphi^e = \rho^e \frac{\partial^2 u_3^e}{\partial t^2} \\ &e_{15} \nabla^2 u_3^e - \in_{11}^e \nabla^2 \varphi^e = 0 \\ &\nabla^2 \psi^e = 0 \end{aligned} \tag{4}$$

where $\nabla^2 = \partial^2/x_1^2 + \partial^2/x_2^2$, t is the time, ρ is the mass density.

The surfaces of piezoelectric/piezomagnetic layers are assumed to be mechanically free, electrically open and magnetically shorted, i.e.,

$$\sigma_{32}^m = D_2^m = B_2^m = 0 \tag{5}$$

at $x_2 = -d^m$ and

$$\sigma_{32}^e = D_2^e = B_2^e = 0 \tag{6}$$

at $x_2 = d^e$. The continuity conditions at the interface of the layers are

$$\begin{aligned} &u_3^m = u_3^e, \quad \varphi^m = \varphi^e, \quad \psi^m = \psi^e \\ &\sigma_{32}^m = \sigma_{32}^e, \quad D_2^m = D_2^e, \quad B_2^m = B_2^e \end{aligned} \tag{7}$$

3. Exact solution

Consider the SH-guided wave propagating in the x_1-direction. The solutions to Eqs. (3) and (4) can be expressed as [15]:

$$\begin{aligned} u_3^\beta(x_1, x_2, t) &= U_3^\beta(x_2) \cos[k(x_1 - ct)] \\ \varphi^\beta(x_1, x_2, t) &= \Phi^\beta(x_2) \cos[k(x_1 - ct)] \\ \psi^\beta(x_1, x_2, t) &= \Psi^\beta(x_2) \cos[k(x_1 - ct)] \end{aligned} \tag{8}$$

where k is the wave number, c is the phase velocity, $U_3^\beta(x_2)$, $\Phi^\beta(x_2)$, and $\Psi^\beta(x_2)$ are undetermined functions, $\beta = m$, e. Substituting Eq. (8) into Eqs. (3) and (4), we can obtain

$$\begin{aligned} &\frac{\partial^2 U_3^m}{\partial x_2^2} - k^2[1 - (c/c_{sh}^m)^2] U_3^m = 0 \\ &\frac{\partial^2 \Phi^m}{\partial x_2^2} - k^2 \Phi^m = 0 \\ &\frac{\partial^2 \Psi^m}{\partial x_2^2} - k^2 \Psi^m = \frac{h_{15}}{\mu_{11}^m} \left(\frac{\partial^2 U_3^m}{\partial x_2^2} - k^2 U_3^m \right) \end{aligned} \tag{9}$$

$$\begin{aligned} &\frac{\partial^2 U_3^e}{\partial x_2^2} - k^2[1 - (c/c_{sh}^e)^2] U_3^e = 0 \\ &\frac{\partial^2 \Phi^e}{\partial x_2^2} - k^2 \Phi^e = \frac{e_{15}}{\in_{11}^e} \left(\frac{\partial^2 U_3^e}{\partial x_2^2} - k^2 U_3^e \right) \\ &\frac{\partial^2 \Psi^e}{\partial x_2^2} - k^2 \Psi^e = 0 \end{aligned} \tag{10}$$

where $c_{sh}^e = \sqrt{\bar{c}_{44}^e/\rho^e}$ and $c_{sh}^m = \sqrt{\bar{c}_{44}^m/\rho^m}$ are the bulk shear wave velocities of piezoelectric and piezomagnetic media,

respectively. $\bar{c}^e_{44} = c^e_{44} + e^2_{15}/\in^e_{11}$ and $\bar{c}^m_{44} = c^m_{44} + h^2_{15}/\mu^m_{11}$ are the stiffened elastic constants with the piezoelectric and piezomagnetic effects, respectively.

For the present problem, we consider two cases, i.e., $c^e_{sh} < c < c^m_{sh}$ and $c^m_{sh} < c < c^e_{sh}$. By solving Eqs. (9) and (10), the component of displacement, the electric potential and the magnetic potential are obtained by

$$\begin{aligned}
u^m_3(x_1,x_2,t) &= [A_1\cosh(k\lambda^m x_2) + A_2\sinh(k\lambda^m x_2)]\cos[k(x_1-ct)] \\
&\quad \text{when } c^e_{sh} < c < c^m_{sh} \\
u^m_3(x_1,x_2,t) &= [A_1\cos(k\lambda^m x_2) + A_2\sin(k\lambda^m x_2)]\cos[k(x_1-ct)] \\
&\quad \text{when } c^m_{sh} < c < c^e_{sh} \\
\varphi^m(x_1,x_2,t) &= [A_3\cosh(kx_2) + A_4\sinh(kx_2)]\cos[k(x_1-ct)] \\
\psi^m(x_1,x_2,t) &= [A_5\cosh(kx_2) + A_6\sinh(kx_2)]\cos[k(x_1-ct)] \\
&\quad + (h_{15}/\mu^m_{11})u^m_3(x_1,x_2,t)
\end{aligned} \tag{11}$$

$$\begin{aligned}
u^e_3(x_1,x_2,t) &= [A_7\cos(k\lambda^e x_2) + A_8\sin(k\lambda^e x_2)]\cos[k(x_1-ct)] \\
&\quad \text{when } c^e_{sh} < c < c^m_{sh} \\
u^e_3(x_1,x_2,t) &= [A_7\cosh(k\lambda^e x_2) + A_8\sinh(k\lambda^e x_2)]\cos[k(x_1-ct)] \\
&\quad \text{when } c^m_{sh} < c < c^e_{sh} \\
\varphi^e(x_1,x_2,t) &= [A_9\cosh(kx_2) + A_{10}\sinh(kx_2)]\cos[k(x_1-ct)] \\
&\quad + (e_{15}/\in^e_{11})u^e_3(x_1,x_2,t) \\
\psi^e(x_1,x_2,t) &= [A_{11}\cosh(kx_2) + A_{12}\sinh(kx_2)]\cos[k(x_1-ct)]
\end{aligned} \tag{12}$$

where $\lambda^m = \sqrt{|1-(c/c^m_{sh})^2|}$, $\lambda^e = \sqrt{|(c/c^e_{sh})^2 - 1|}$.

Substituting Eqs. (11) and (12) into Eqs. (1) and (2), we can obtain

$$\begin{aligned}
\sigma^m_{32} &= k\{\bar{c}^m_{44}\lambda^m[-A_1\sinh(k\lambda^m x_2) + A_2\cosh(k\lambda^m x_2)] \\
&\quad + h_{15}[A_5\sinh(kx_2) + A_6\cosh(kx_2)]\}\cos[k(x_1-ct)] \\
D^m_2 &= -k\in^m_{11}[A_3\sinh(kx_2) + A_4\cosh(kx_2)]\cos[k(x_1-ct)] \\
B^m_2 &= -k\mu^m_{11}[A_5\sinh(kx_2) + A_6\cosh(kx_2)]\cos[k(x_1-ct)]
\end{aligned} \tag{13}$$

$$\begin{aligned}
\sigma^e_{32} &= k\{\bar{c}^e_{44}\lambda^e[A_7\sin(k\lambda^e x_2) + A_8\cos(k\lambda^e x_2)] \\
&\quad + e_{15}[A_9\sinh(kx_2) + A_{10}\cosh(kx_2)]\}\cos[k(x_1-ct)] \\
D^e_2 &= -k\in^e_{11}[A_9\sinh(kx_2) + A_{10}\cosh(kx_2)]\cos[k(x_1-ct)] \\
B^e_2 &= -k\mu^e_{11}[A_{11}\sinh(kx_2) + A_{12}\cosh(kx_2)]\cos[k(x_1-ct)]
\end{aligned} \tag{14}$$

for $c^e_{sh} < c < c^m_{sh}$ and

$$\begin{aligned}
\sigma^m_{32} &= k\{\bar{c}^m_{44}\lambda^m[-A_1\sin(k\lambda^m x_2) + A_2\cos(k\lambda^m x_2)] \\
&\quad + h_{15}[A_5\sinh(kx_2) + A_6\cosh(kx_2)]\}\cos[k(x_1-ct)] \\
D^m_2 &= -k\in^m_{11}[A_3\sinh(kx_2) + A_4\cosh(kx_2)]\cos[k(x_1-ct)] \\
B^m_2 &= -k\mu^m_{11}[A_5\sinh(kx_2) + A_6\cosh(kx_2)]\cos[k(x_1-ct)]
\end{aligned} \tag{15}$$

$$\begin{aligned}
\sigma^e_{32} &= k\{\bar{c}^e_{44}\lambda^e[A_7\sinh(k\lambda^e x_2) + A_8\cosh(k\lambda^e x_2)] \\
&\quad + e_{15}[A_9\sinh(kx_2) + A_{10}\cosh(kx_2)]\}\cos[k(x_1-ct)] \\
D^e_2 &= -k\in^e_{11}[A_9\sinh(kx_2) + A_{10}\cosh(kx_2)]\cos[k(x_1-ct)] \\
B^e_2 &= -k\mu^e_{11}[A_{11}\sinh(kx_2) + A_{12}\cosh(kx_2)]\cos[k(x_1-ct)]
\end{aligned} \tag{16}$$

for $c^m_{sh} < c < c^e_{sh}$

4. Dispersion relation

In this section, we make use of the solutions derived in the previous section and also the boundary conditions (5), (6) and the continuity conditions (7) to obtain the dispersion relation. Substituting Eqs. (11)–(16) into Eqs. (5)–(7), we can obtain

$$\begin{aligned}
&\bar{c}^m_{44}\lambda^m[A_1\sinh(k\lambda^m d^m) + A_2\cosh(k\lambda^m d^m)] \\
&\quad - h_{15}[A_5\sinh(kd^m) - A_6\cosh(kd^m)] = 0 \\
&A_3\sinh(kd^m) - A_4\cosh(kd^m) = 0 \\
&A_5\sinh(kd^m) - A_6\cosh(kd^m) = 0 \\
&\bar{c}^e_{44}\lambda^e[A_7\sin(k\lambda^e d^e) + A_8\cos(k\lambda^e d^e)] \\
&\quad + e_{15}[A_9\sinh(kd^e) + A_{10}\cosh(kd^e)] = 0 \\
&A_9\sinh(kd^e) + A_{10}\cosh(kd^e) = 0 \\
&A_{11}\sinh(kd^e) + A_{12}\cosh(kd^e) = 0 \\
&A_1 - A_7 = 0 \\
&(e_{15}/\in^e_{11})A_7 - A_3 + A_9 = 0 \\
&(h_{15}/\mu^m_{11})A_1 - A_{11} + A_5 = 0 \\
&\bar{c}^m_{44}\lambda^m A_2 - \bar{c}^e_{44}\lambda^e A_8 + h_{15}A_6 - e_{15}A_{10} = 0 \\
&\in^m_{11}A_4 - \in^e_{11}A_{10} = 0 \\
&\mu^e_{11}A_{12} - \mu^m_{11}C_6 = 0
\end{aligned} \tag{17}$$

for $c^e_{sh} < c < c^m_{sh}$ and

$$\begin{aligned}
&\bar{c}^m_{44}\lambda^m[A_1\sin(k\lambda^m d^m) + A_2\cos(k\lambda^m d^m)] - h_{15}[A_5\sinh(kd^m) \\
&\quad - A_6\cosh(kd^m)] = 0 \\
&A_3\sinh(kd^m) - A_4\cosh(kd^m) = 0 \\
&A_5\sinh(kd^m) - A_6\cosh(kd^m) = 0 \\
&\bar{c}^e_{44}\lambda^e[A_7\sinh(k\lambda^e d^e) + A_8\cosh(k\lambda^e d^e)] + e_{15}[A_9\sinh(kd^e) \\
&\quad + A_{10}\cosh(kd^e)] = 0 \\
&A_9\sinh(kd^e) + A_{10}\cosh(kd^e) = 0 \\
&A_{11}\sinh(kd^e) + A_{12}\cosh(kd^e) = 0 \\
&A_1 - A_7 = 0 \\
&(e_{15}/\in^e_{11})A_7 - A_3 + A_9 = 0 \\
&(h_{15}/\mu^m_{11})A_1 - A_{11} + A_5 = 0 \\
&\bar{c}^m_{44}\lambda^m A_2 - \bar{c}^e_{44}\lambda^e A_8 + h_{15}A_6 - e_{15}A_{10} = 0 \\
&\in^m_{11}A_4 - \in^e_{11}A_{10} = 0 \\
&\mu^e_{11}A_{12} - \mu^m_{11}C_6 = 0
\end{aligned} \tag{18}$$

Table 1
Material properties used in the computation.

	$CoFe_2O_4$	$BaTiO_3$	PZT-4
$c_{44}(\times 10^9 N/m^2)$	45.3	44	25.6
$\rho(\times 10^3 kg/m^3)$	5.3	5.7	7.5
$\varepsilon_{11}(\times 10^{-9} C^2/Nm^2)$	0.08	9.86	6.45
$\mu_{11}(\times 10^{-6} Ns^2/C^2)$	157	5	5
$e_{15}(C/m^2)$	–	11.4	12.7
$h_{15}(N/Am)$	550	–	–
$C_{sh}(m/s)$	2985.08	3167.28	2597.59

for $c_{sh}^m < c < c_{sh}^e$

Both are twelve homogeneous linear algebraic equations for the undetermined coefficients $A_i (i = 1, 2, \cdots, 12)$. By letting the determinants of the coefficient matrices in Eqs. (17) and (18) be zero, i.e., $|A_{ij}| = 0 (i, j = 1, 2, \cdots, 12)$, the dispersion relation is obtained.

5. Numerical results

Using the derived dispersion relations in the previous section, SH-guided wave propagations in $BaTiO_3/CoFe_2O_4$ and PZT-4/$CoFe_2O_4$ coupled plates are discussed. And the phase velocities are plotted to illustrate the dispersion behaviors. The materials used in the numerical calculation are listed in Table 1 [16]. For the convenience of the following discussions, the bulk shear wave velocities of piezoelectric material and piezomagnetic material are also listed in Table 1. In the following figures, the horizontal axis represents the non-dimensional wave number $K = kd^m/2\pi$, and the vertical axis represents the phase velocity.

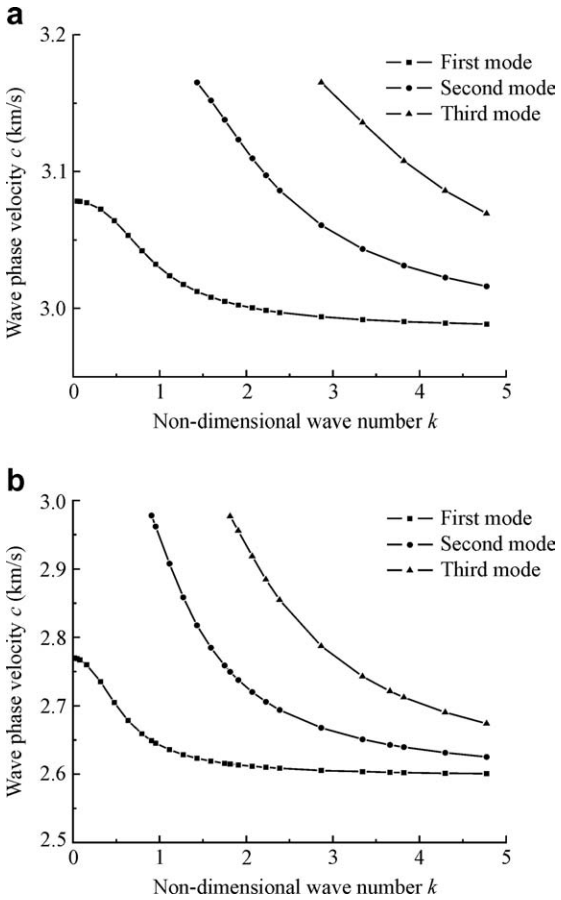

Fig. 2. Dispersion curves of the first three modes for the piezoelectric/piezomagnetic plate. (a) $BaTiO_3/CoFe_2O_4$ plate; (b) PZT-4/$CoFe_2O_4$ plate.

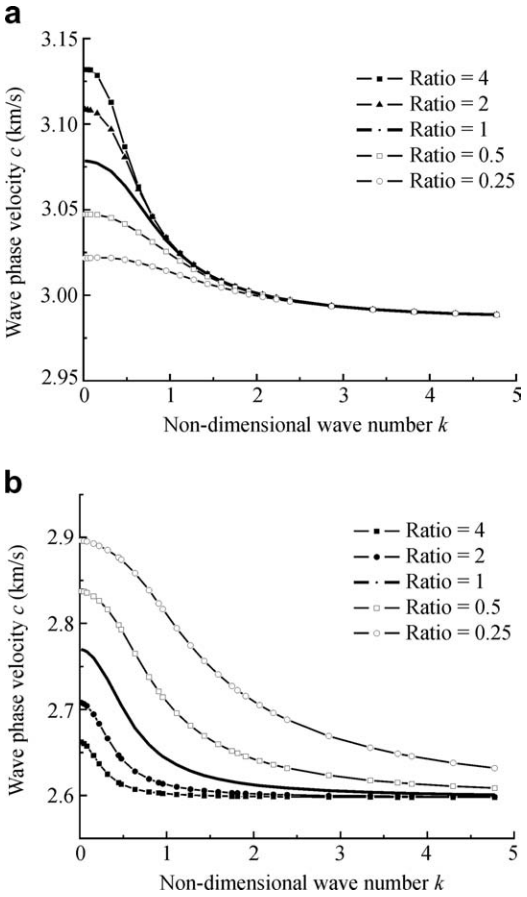

Fig. 3. Comparison of the first mode for the piezoelectric/piezomagnetic plate with different thickness ratios. (a) $BaTiO_3/CoFe_2O_4$ plate; (b) PZT-4/$CoFe_2O_4$ plate.

The dispersion curves of the first three modes for $BaTiO_3/CoFe_2O_4$ and PZT-4/$CoFe_2O_4$ coupled plates are shown in Fig. 2(a and b), respectively. And the thickness ratio of piezoelectric/piezomagnetic layers is taken as 1. It can be seen from Fig. 2(a and b) that the phase velocity approaches the bulk shear wave velocity of the piezoelectric material with the increase in the wave number for different modes. It means that the phase velocity approaches the smaller bulk shear wave velocity of the material in the system.

The comparison of the first mode for different thickness ratios of $BaTiO_3/CoFe_2O_4$ and PZT-4/$CoFe_2O_4$ coupled plates is shown in Fig. 3(a and b). And the comparison of the second mode is shown in Fig. 4(a and b). It can be seen from Fig. 3(a) and Fig. 4(a) that the phase velocity decreases with the decrease in the thickness ratios for the first mode. The states of the second

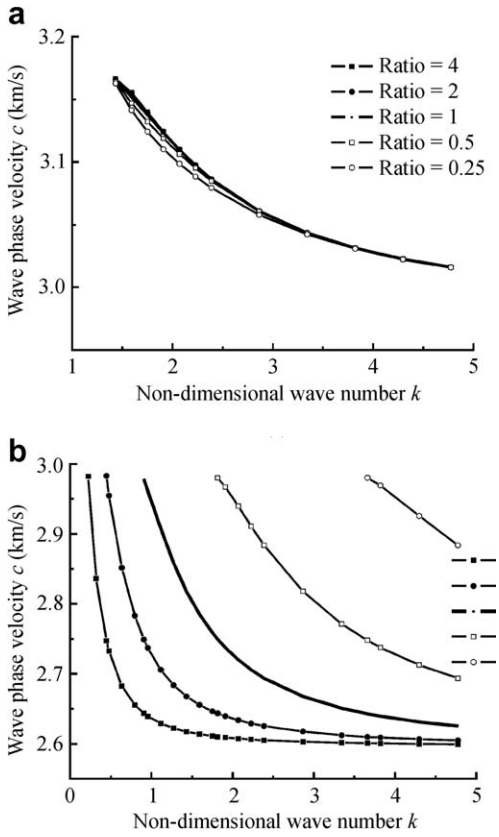

Fig. 4. Comparison of the second mode for the piezoelectric/piezomagnetic plate with different thickness ratios. (a) $BaTiO_3/CoFe_2O_4$ plate; (b) PZT-4/$CoFe_2O_4$ plate.

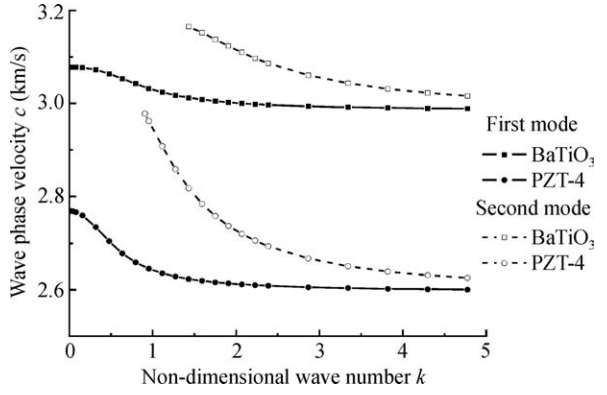

Fig. 5. Comparison of the first two modes for the plates with different piezoelectric layers.

mode are contrary to the first mode shown in Fig. 3(b) and Fig. 4(b). It is observed that the phase velocity has great discrepancy for the smaller wave number, and when the wave number becomes larger, the discrepancy will decrease, which is due to the fact that the bulk shear wave velocity of $BaTiO_3$ is larger than that of $CoFe_2O_4$, and the bulk shear wave velocity of PZT-4 is smaller than that of $CoFe_2O_4$.

The influence of different piezoelectric material properties on the first and second modes is shown in Fig. 5, where the thickness ratio of piezoelectric/piezomagnetic material is taken as 1. From Fig. 5, it can be seen that the phase velocities have the relation: $c_{BaTiO_3/CoFe_2O_4} > c_{PZT-4/CoFe_2O_4}$ for a given wave number. It means that the larger the bulk shear wave velocity of a piezoelectric layer, the larger is the phase velocity.

6. Conclusions

The propagation of the SH-guided wave in the piezoelectric/piezomagnetic-layered plates is studied in this paper. The exact solution of the problem is derived. The numerical results show that the phase velocity approaches the smaller bulk shear wave velocity of the material in the system with the increase in the wave number for different modes. The thickness ratios have a great effect on the dispersion behavior when the wave number is smaller, and with the increase of wave number, the discrepancy will decrease. The properties of the piezoelectric material have evident effect on the dispersion curves, and the larger the bulk shear wave velocity of a piezoelectric layer, the larger is the phase velocity. The results of this paper can offer some fundamental theory to the application of piezoelectric/piezomagnetic composites or structures.

Acknowledgement

This work was supported by the National Natural Science Foundation of China (Grant No. 10472074).

References

[1] Du JK, Shen YP, Ye DY, et al. Scattering of anti-plane shear waves by a partially debonded magneto-electro-elastic circular cylindrical inhomogeneity. Int J Eng Sci 2004;42(9):887–913.
[2] Meguid SA, Wang XD. An elastodynamic analysis of interacting inhomogeneities in advanced composites. Mech Mater 2000;32(12):797–805.
[3] Hirotaka S, Shindo Y. Multiple scattering of plane elastic wave in a fiber-reinforced composite medium with graded interfacial layers. Int J Solids Struct 2001;38(15):2549–71.
[4] Van Suchtelen J. Product properties: a new application of composite materials. Philips Res Rep 1972;27(1):28–37.
[5] Huang JH, Liu HK, Dai WL. The optimized fiber volume fraction for magnetoelectric coupling effect in piezoelectric-piezomagnetic continuous fiber reinforced composites. Int J Eng Sci 2000;38:1207–17.
[6] Srinivasan G, Rasmussen ET, Gallegos J, et al. Magnetoelectric bilayer and multilayer structures of magnetostrictive and piezoelectric oxides. Phys Rev B 2001;64(21):214408-1–6.
[7] Srinivasan G, Laletsin VM, Hayes R, et al. Giant magnetoelectric effects in layered composites of nickel zinc ferrite and lead zirconate titanate. Solid State Commun 2002;124(10–11):373–8.
[8] Mazumder S, Battacharyya GS. Magnetoelectric behavior in in situ grown piezoelectric and piezomagnetic composite-phase system. Mater Res Bull 2003;38(2):303–10.
[9] Nersessian N, Or SW, Carman GP. Magnetoelectric behavior of Terfenol-D composite and lead zirconate titanate ceramic laminates. IEEE Trans Magnet 2004;40(4):2646–8.
[10] Ren SQ, Weng LQ, Song SH, et al. $BaTiO_3/CoFe_2O_4$ particulate composites with large high frequency magnetoelectric response. J Mater Sci 2005;40(16):4375–8.

[11] Wang Q, Quek ST, Varadan VK. Love waves in piezoelectric coupled solid media. Smart Mater Struct 2001;10(2):380–8.
[12] Fan H, Yang JS, Xu LM. Antiplane piezoelectric surface waves over a ceramic half-space with an imperfectly bonded layer. IEEE Trans Ultrason Ferroelec Freq Contr 2006;53(9):1695–8.
[13] Du JK, Jin X, Wang J. Love wave propagation in layered magneto-electro-elastic structures with initial stress. Acta Mech 2007;192(1–4):169–89.
[14] Soh AK, Liu JX. Interfacial shear horizontal waves in a piezoelectric-piezomagnetic bi-material. Philos Mag Lett 2006;86(1):31–5.
[15] Peng F, Hu SY. Investigation of shear horizontal acoustics wave in an inhomogeneous magnetoelectroelastic plate. Key Eng Mater 2006;306–308:1217–22.
[16] Chen JY, Pan E, Chen HL. Wave propagation in magneto-electro-elastic multilayered plates. Int J Solids Struct 2007;44(3–4): 1073–85.